JACS
JOURNAL OF THE AMERICAN CHEMICAL SOCIETY
Article
pubs.acs.org/JACS

Water Oxidation by the $[Co_4O_4(OAc)_4(py)_4]^+$ Cubium is Initiated by OH^- Addition

Paul F. Smith,[†] Liam Hunt,[†] Anders B. Laursen,[†] Viral Sagar,[†] Shivam Kaushik,[†] Karin U. D. Calvinho,[†] Gabriele Marotta,[‡] Edoardo Mosconi,[‡] Filippo De Angelis,[‡] and G. Charles Dismukes*[,†]

[†]Department of Chemistry and Chemical Biology, Rutgers, the State University of New Jersey, 610 Taylor Road, Piscataway, New Jersey 08854, United States

[‡]Computational Laboratory for Hybrid/Organic Photovoltaics (CLHYO), Istituto CNR di Scienze e Tecnologie Molecolari (ISTM-CNR), Via Elce di Sotto 8, Perugia 06123, Italy

Supporting Information

ABSTRACT: The cobalt cubium $Co_4O_4(OAc)_4(py)_4(ClO_4)$ ($\mathbf{1A}^+$) containing the mixed valence $[Co_4O_4]^{5+}$ core is shown by multiple spectroscopic methods to react with hydroxide (OH^-) but not with water molecules to produce O_2. The yield of reaction products is stoichiometric (>99.5%): $4\mathbf{1A}^+ + 4OH^- \rightarrow O_2 + 2H_2O + 4\mathbf{1A}$. By contrast, the structurally homologous cubium $Co_4O_4(trans\text{-}OAc)_2(bpy)_4(ClO_4)_3$, $\mathbf{1B}(ClO_4)_3$, produces no O_2. EPR/NMR spectroscopies show clean conversion to cubane **1A** during O_2 evolution with no Co^{2+} or Co_3O_4 side products. Mass spectrometry of the reaction between isotopically labeled μ-^{16}O(bridging-oxo) $\mathbf{1A}^+$ and ^{18}O-bicarbonate/water shows (1) no exchange of ^{18}O into the bridging oxos of $\mathbf{1A}^+$, and (2) $^{36}O_2$ is the major product, thus requiring two OH^- in the reactive intermediate. DFT calculations of solvated intermediates suggest that addition of two OH^- to $\mathbf{1A}^+$ via OH^- insertion into Co−OAc bonds is energetically favored, followed by outer-sphere oxidation to intermediate $[\mathbf{1A}(OH)_2]^0$. The absence of O_2 production by cubium $\mathbf{1B}^{3+}$ indicates the reactive intermediate derived from $\mathbf{1A}^+$ requires *gem*-1,1-dihydoxo stereochemistry to perform O−O bond formation. Outer-sphere oxidation of this intermediate by 2 equiv of $\mathbf{1A}^+$ accounts for the final stoichiometry. Collectively, these results and recent literature (*Faraday Discuss.*, doi:10.1039/C5FD00076A and *J. Am. Chem. Soc.* **2015**, *137*, 12865−12872) validate the $[Co_4O_4]^{4+/5+}$ cubane core as an intrinsic catalyst for oxidation of hydroxide by an inner-sphere mechanism.

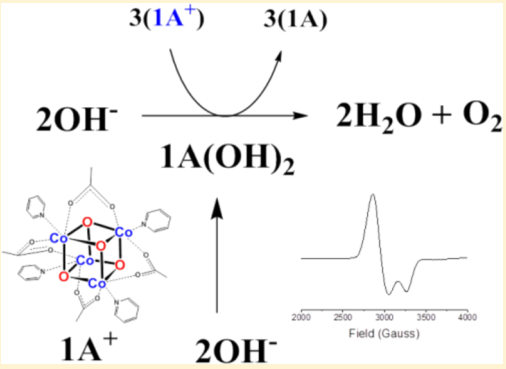

INTRODUCTION

Sustainable production of hydrogenic fuels requires an abundant source of hydrogen. Water is the ideal source of hydrogen, but must first be cleaved by an energetic process in which four strong O−H bonds are broken. Toward this goal, several heterogeneous cobalt oxide catalysts for electrochemical water oxidation have been reported[1−6] and widely applied.[7−18] Rational design of heterogeneous catalysts is difficult, and can significantly benefit from understanding gained from simpler homogeneous catalysts. To better understand their basis for catalysis, several molecular cobalt clusters have been synthesized and reported to be active homogeneous catalysts.[19−29] Of interest from these are clusters containing a Co_4O_4 "cubane" core,[30,31] which is a recurring structural theme among biological and synthetic water oxidation catalysts.[32,33] Many studies have described the properties[34−47] of $Co_4O_4(OAc)_4(py)_4$, **1A**, and $[Co_4O_4(OAc)_2(bpy)_4](ClO_4)_2$, $\mathbf{1B}^{2+}(ClO_4)_2$ (Scheme 1).

The synthesis and characterization of cubane **1A** has an extensive history. Oxidation of Co^{2+} acetate by peroxide or peracetic acid was known to give a complex, equilibrating, reaction mixture, until the addition of pyridine allowed isolation of dimeric and trimeric cobalt cations.[48] Cubane **1A**, which is neutral and has high solubility in many solvents, escaped detection from this synthesis until many years later.[47] Other studies targeted formation of the cubane using alternate

Scheme 1. Cubanes: $Co_4O_4(OAc)_4(py)_4$, 1A, and $[Co_4O_4(OAc)_2(bpy)_4]^{2+}$, $\mathbf{1B}^{2+}$

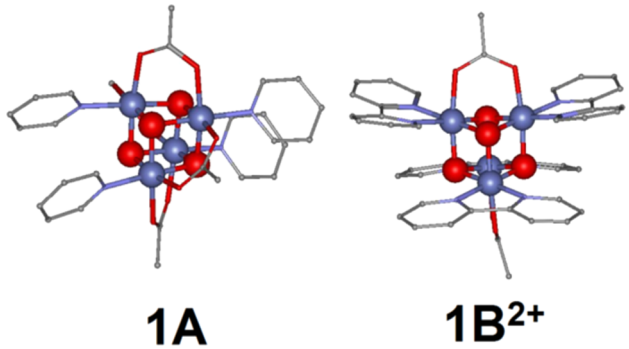

Received: August 28, 2015
Published: November 22, 2015

© 2015 American Chemical Society

DOI: 10.1021/jacs.5b09152
J. Am. Chem. Soc. 2015, 137, 15460−15468

carboxylates and substituted pyridines to shift the equilibrium,[38] although the general synthetic method remained similar. These later reports served as the basis for the preparation of **1A** by several groups including ourselves, who all showed **1A** (and close analogues) to oxidize water (pH 6–8) photochemically and electrochemically.[49−55] DFT calculations suggested energetically accessible routes to catalytic O_2 evolution from model Co_4O_4 cubanes (terminated by water ligands), although nucleophilic attack,[56] cross-coupling,[57] and geminal coupling[58] mechanisms have been proposed.

Recently, Nocera et al. provided strong evidence that Co^{2+} impurities remaining from synthesis form the main catalyst when oxidized in phosphate buffer either electrochemically or via a Ru^{3+} photo-oxidant.[59] From that report, pristine **1A** was found inactive for electrochemical water oxidation. While the pure compound was photochemically active, catalysis was ascribed to decomposition products. More recently, Bonchio et al. showed by kinetic studies that **1A** minus an acetate ligand is the most likely intrinsic water oxidation catalyst in the photochemical assay.[60] This derivative is accessible by aging **1A** in water, and additionally shows electrochemical activity.

Herein, we show that the oxidized cubium, $\mathbf{1A(ClO_4)}$, reacts with OH^- to release O_2 spontaneously without an external oxidant, light, or electrolysis potential. The Co_4O_4 cubane core serves two roles in O_2 evolution: intact $\mathbf{1A^+}$ serves as an outer-sphere oxidant and as precatalyst that forms the reactive intermediate by association with hydroxide. Evidence from mass spectrometry, NMR, and DFT calculations of energy minimized structures implicates formation of an association complex via insertion of OH^- into a $Co{-}OAc^-$ bond of $\mathbf{1A^+}$, forming the first precatalytic intermediate, $[\mathbf{1A(OH)}]$. This intermediate cannot be oxidized by another $\mathbf{1A^+}$ molecule until a second OH^- inserts in another $Co{-}OAc^-$ bond, yielding $[\mathbf{1A(OH)_2}]^0$. Isotopic labeling studies establish that terminally coordinated hydroxide ions, but not bridging oxos within the cubane, are the substrates that form O_2. Our results on the reactivity of $\mathbf{1A^+}$ with OH^- agree with those in a recent report that appeared while this manuscript was in review[61] and also provide additional kinetic data that are described in the discussion. Our results are further extended herein by parallel studies of a structurally homologous cubium $\mathbf{1B^{3+}}$ having only 2 carboxylate chelates in trans configuration and 4 bpy replacing py (Scheme 1). In contrast to $\mathbf{1A^+}$, the isolated perchlorate derivative, $\mathbf{1B(ClO_4)_3}$, fails to produce O_2 when reacted with OH^-, suggesting the stereochemistry of the associative hydroxide intermediate involves the *gem*-1,1-dihydroxo formation from $\mathbf{1A^+}$ as precatalyst.

RESULTS

Reduction of $1A^+$ in the Presence of Hydroxide. After performing column chromatography on samples of cubane **1A**, we observed no noticeable water oxidation current above a background glassy carbon electrode in buffered water (0.1 M phosphate buffer at pH 7) (Figure 1), consistent with the pure samples isolated by several groups.[59−61] We adapted two literature procedures to synthesize $\mathbf{1A^+}$: (1) electrochemical oxidation,[44] yielding the ClO_4^- salt; and (2) chemical oxidation,[59] yielding the PF_6^- salt. The following results are all consistent regardless of preparation method.

The EPR spectrum of $\mathbf{1A^+}$ dissolved in water/acetonitrile glass forming solvent is comparable to the initial report of Britt et al.[44] (Figure 2). Specifically, the line shape and Curie temperature dependence indicate a spin $S = 1/2$ ground state

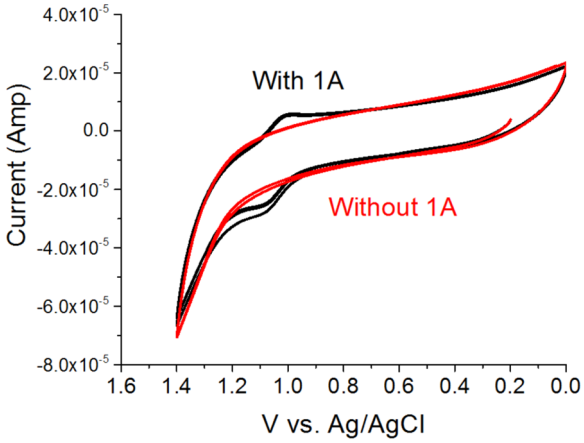

Figure 1. Cyclic voltammograms at a glassy carbon electrode in aqueous phosphate (0.1 M, pH 7) with and without 500 μM of **1A**.

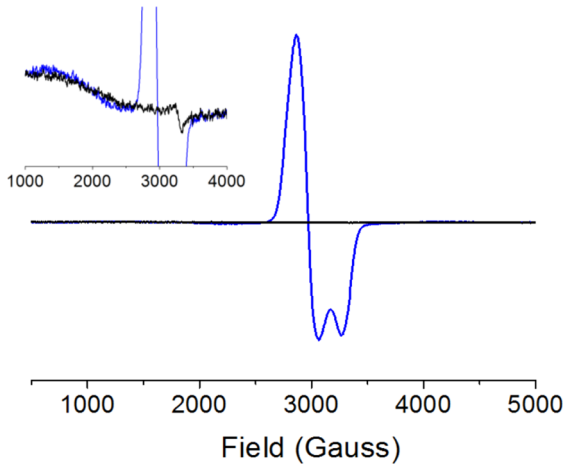

Figure 2. EPR spectrum at 10 K of 15 mM CH_3CN solutions of $\mathbf{1A(ClO_4)}$ without (blue) and with (black) 0.1 M NaOH. Inset: 10× expansion from another independent trial. Samples were not degassed.

with an axial g tensor, $g_{\parallel} = 2.06$ and $g_{\perp} = 2.28$. There is no resolved hyperfine structure from ^{59}Co ($I = 7/2$, 100% n.a.) and no features at lower field where species of higher spin multiplicity can absorb. The sample (up to 15 mM concentration) exhibits no EPR signal for Co^{2+} or for that matter any paramagnetic impurity.

$\mathbf{1A^+}$ as isolated is not water-soluble, but dissolves in aqueous solutions of NaOH, *N*-butylammonium hydroxide, sodium bicarbonate, and sodium carbonate. As monitored by EPR and UV–vis spectroscopies, the addition of any of these hydroxide sources to $\mathbf{1A^+}/CH_3CN$ solutions results in reduction to diamagnetic **1A** (Figures 2 and 3, respectively). Bubbles are released upon this reaction and confirmed as O_2 by Clark electrode, gas chromatography, and membrane inlet mass spectrometry (vide infra).

UV–vis titrations indicated 1:1 stoichiometry of cubium to hydroxide completes the reaction (Figure 3, inset, and Figure S1). Given that $\mathbf{1A^+}$ precipitates from water in the last step of synthesis, no reduction in the presence of water was anticipated, as confirmed by control experiments over the time scale of several minutes (Figure S1). Control measurements without $\mathbf{1A^+}$ or OH^- produced no measurable O_2 in all of these trials.

DOI: 10.1021/jacs.5b09152
J. Am. Chem. Soc. 2015, 137, 15460−15468

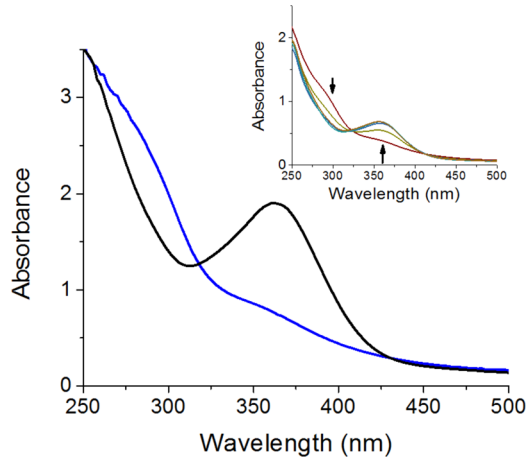

Figure 3. UV−vis spectra of 170 μM CH_3CN solutions of $\mathbf{1A}^+$ (blue) and **1A** (black). Inset: Spectral changes following addition of 4× 0.5 equiv aliquots of OH^- to 60 μM of $\mathbf{1A}^+$, showing two isosbestic points and no observable intermediates.

Gas chromatography was used to quantify the O_2 produced upon complete dissolution of 2−2.5 μmol of $\mathbf{1A(ClO_4)}$ in 10 equiv of aqueous NaOH. The amount of O_2 produced was quantitatively consistent with reduction of $4Co^{4+}$ to $4Co^{3+}$ (O_2:$\mathbf{1A}^+$ ratio of 0.27 ± 0.03). NMR integration of the product solution was quantitatively consistent with formation of **1A** as the sole product (99.5% recovery). Consistent with this result, EPR spectroscopy of solutions of the reaction product showed no identifiable paramagnetic Co^{2+} (Figure 2, black trace), suggesting only Co^{3+} in the product. We did not observe CO_2 or CO in the product gas above GC detection (<10 nmol, 0.5%), consistent with no oxidation of substrates other than OH^-. Hence, the reaction stoichiometry is given by eq 1:

$$4\mathbf{1A}^+ + 4OH^- \rightarrow O_2 + 4\mathbf{1A} + 2H_2O \quad (1)$$

As determined by Clark electrode, the method of initial rates indicates that the O_2 evolution reaction is first order in both cubium and OH^- when using one limiting reactant (pseudo-first order conditions) (Figure 4). Rates decrease from linear

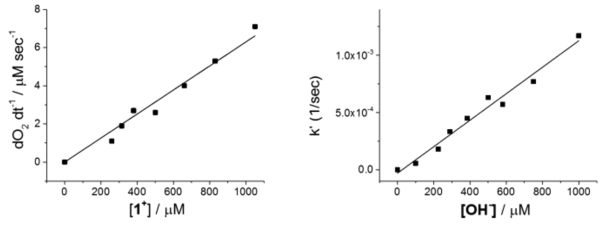

Figure 4. Left: Initial rate of O_2 production as a function of initial [$\mathbf{1A}^+$] in excess NaOH (40 mM). Right: Pseudo-first-order rate constants as a function of OH^- in excess [$\mathbf{1A}^+$] (2 mM).

dependence at [OH^-] > 1 mM. A plot of the pseudo-first order constants versus [OH^-] gives the bimolecular rate constant k = 1.1 $(M\ s)^{-1}$ for the reaction, eq 2.

$$d[O_2]/dt = k[\mathbf{1A}^+][OH^-],\ k = 1.1\ M^{-1}\ s^{-1} \quad (2)$$

The fates of the OAc^- and py ligands after reaction were monitored by ^1H NMR spectroscopy. The pyridine region of the ^1H NMR spectrum of $\mathbf{1A}^+$ in CD_3CN consists of a single broad peak, due to the paramagnetic broadening of this material (Figure 5A). Upon addition of 4 equiv of hydroxide

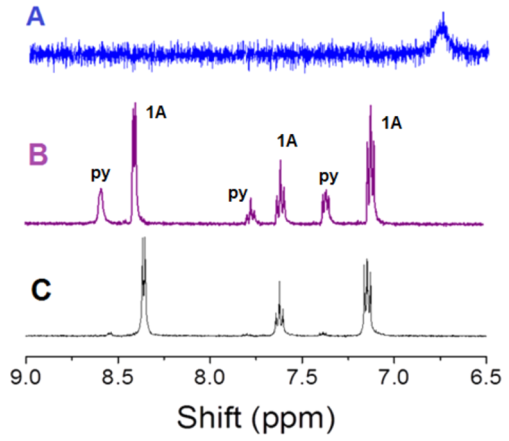

Figure 5. ^1H NMR spectra of CD_3CN solutions of (A) $\mathbf{1A}^+$ (blue), (B) a mixture of pyridine and **1A** (purple), and (C) the reaction of 1.5 mM $\mathbf{1A}^+$ with 4 equiv of OH^- (black).

(Figure 5C), the resulting spectrum most prominently contains sharp pyridine resonances that match those of **1A** (Figure 5B). Free pyridine and acetate resonances are observed above the NMR detection limit only when using 1.5 mM or higher cubium concentrations (Figure 5C and Figure S2, respectively). Integration of the free:bound ligand ratio indicated 99.5% of ligands (py and OAc) remain bound to cubane **1A**. Free ligands were not seen in previous studies, which utilized cubane concentrations 5−150× less than that used here.[49,54] Collectively, these data suggest that the stoichiometric reduction reaction between cubium and OH^- proceeds without net ligand loss.

High-resolution mass spectrometry of the reaction products using ^{18}O-hydroxide were conducted to determine the origin of the evolved O_2. After dissolving $\mathbf{1A}^+$ in water (79% ^{18}O) containing 0.3 M sodium bicarbonate (100% ^{18}O), the product solution was analyzed by ESI-QTOF-MS in positive ion mode (no negative ion peaks were observed). The MS spectrum (Figure S3) consisted of peaks at 875 m/z (**1A** + $^{23}Na)^+$, 853 (**1AH**)$^+$, 774 (**1A**-py + H^+), 796 (**1A**-py + $^{23}Na^+$), and 793 (**1A**-OAc)$^+$, and no evidence for ^{18}O incorporation into any fragment. Peaks at M+1 and M+2 for each fragment quantitatively account for the natural abundance of ^{13}C in each product (±1%) and were completely consistent with control MS spectra of **1A** in either ^{16}O or ^{18}O water, with and without added ^{18}O bicarbonate (Figures S3−S5). Hence, **1A** is inert to μ-oxo/water exchange, and throughout the course of the O_2 evolving reaction of $\mathbf{1A}^+$ in bicarbonate no ^{18}O was incorporated into the bridging oxos. This outcome dictates that the oxygen atoms in the product O_2 must both originate from hydroxide, a prediction that was subsequently confirmed by membrane inlet mass spectrometry (MIMS).

MIMS allows real-time detection of O_2 produced from dissolution of $\mathbf{1A}^+$ in alkaline solution. The O_2 product from the dissolution of $\mathbf{1A}^+$ with ^{18}O bicarbonate in 97% ^{18}O-water under purged-Ar atmosphere was comprised of 75% $^{36}O_2$, 19% $^{34}O_2$, and 6% $^{32}O_2$ (Figure 6). In our setup, performing identical experiments with higher amounts of background air in the MS causes the intensity of the $^{34}O_2$ signal to increase in direct correlation with a decrease in the $^{36}O_2$ signal (Figure S6). Therefore, a portion of the $^{34}O_2$ signal arises from scrambling of $^{36}O_2$ with atmospheric $^{32}O_2$ via $^{32}O_2 + {}^{36}O_2 \rightarrow 2{}^{34}O_2$.

DOI: 10.1021/jacs.5b09152
J. Am. Chem. Soc. 2015, 137, 15460−15468

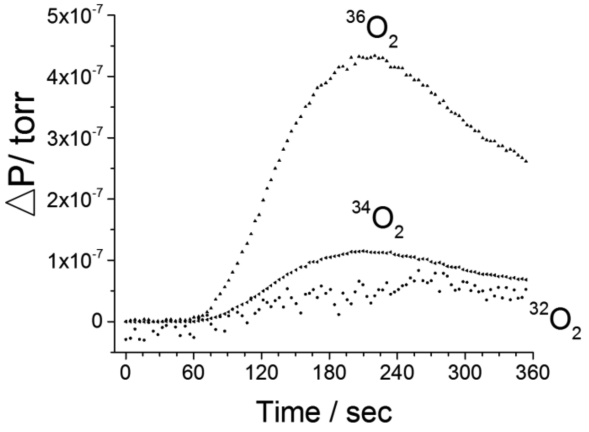

Figure 6. MIMS data for the reaction of $\mathbf{1A}^+$ (8 mM) with ^{18}O labeled sodium bicarbonate (0.15 M) in 97% ^{18}O water.

Extrapolation to zero background air gives >81% $^{36}O_2$ as a lower bound percentage of the product O_2 yield.

The cumulative results suggest that the O_2 evolution reaction occurs by addition of OH^- without loss of ligands, and that these sites are eventually evolved as O_2 following oxidation by the $\mathbf{1A}^+/\mathbf{1A}$ couple (1.25 V vs NHE). $\mathbf{1A}^+$ thus has unique, dual functionality depending on ligation, serving both as outer-sphere oxidant and as precatalyst.

DFT Calculations of Hydroxide Exchange. For further insights, we pursued DFT calculations to predict the energetics of formation of intermediates with progressive addition or exchange of ligands for water and hydroxide. Calculations were performed on an extended set of molecules (see the Supporting Information) in acetonitrile solution on the geometries optimized in vacuo. To calculate the energetics of different reaction pathways, we employed fragments (OH^-, OAc^-, and Py) solvated by four water molecules. Additional calculations employing four explicit water molecules in the solvation sphere of the reaction sites have been performed to further check the stability of different reaction intermediates. The calculated oxidation potential of the $\mathbf{1A}/\mathbf{1A}^+$ couple is 5.57 eV, vertical line in Figure 7, which nicely compares to the experimental oxidation potential of ~5.7 eV versus vacuum (i.e., 1.25 V vs NHE + 4.44 eV).

We consider two possible binding sites, that is, exchange of OH^- with a pyridine or insertion of OH^- into a Co−OAc bond, to form a complex that is stabilized by a hydrogen bond to the monodentate acetate ligand, shown in Figure 7. Crystallographic evidence for intramolecular H bonding of this type has been directly observed in Mn_4O_4-cubanes,[62] and correlated with water oxidation activity in cobalt hangman complexes.[22] OH^- addition to the neutral cubane **1A**, forming anion $[\mathbf{1A}(OH)]^-$, is thermodynamically unfavored (+0.36 to 0.46 eV, at $^-$OAc and Py sites; Figure 7). For the oxidized cubium $\mathbf{1A}^+$, the lowest energy pathway for OH^- addition is the associative product $[\mathbf{1A}(OH)]$, rather than by pyridine exchange (−0.92 vs −0.63 eV, respectively, Figure 7). Intermediate $[\mathbf{1A}(OH)]$ has also been found lowest in energy by Li and Siegbahn[56] at the identical $Co_4(3,3,3,4)$ level.

Li and Siegbahn assumed conditions of 1.43 V oxidizing potential[56] and calculated that $[\mathbf{1A}(OH)]^0$ is further oxidized to $Co_4(3,3,4,4)$. In their calculation, this derivative undergoes O−O bond formation via water nucleophilic attack. In our calculations, which limit the oxidizing potential to 1.25 V (equal to the couple $\mathbf{1A}/\mathbf{1A}^+$), oxidation of $[\mathbf{1A}(OH)]^0$ is unfavorable by +0.27 eV, and proton transfer from the hydroxide to the acetate ligand is highly unfavorable by +1.13 eV. We thus considered a second OH^-/H_2O binding as the next step in the reaction mechanism (Figure 8). Our

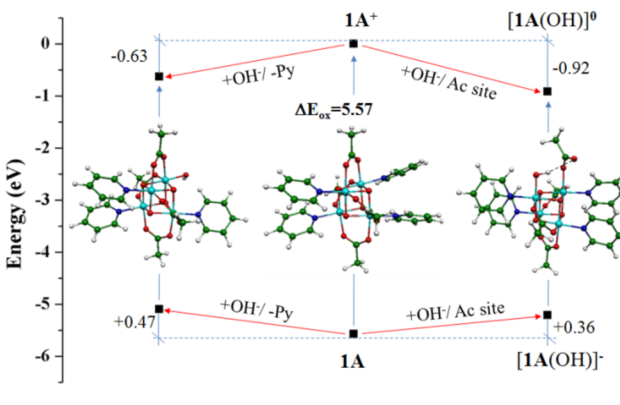

Figure 7. Stereochemistry and energetics from DFT calculations of the first OH^- binding intermediates for both **1A** (unfavorable) and $\mathbf{1A}^+$ (favorable). The calculated $\mathbf{1A}/\mathbf{1A}^+$ oxidation potential is also reported.

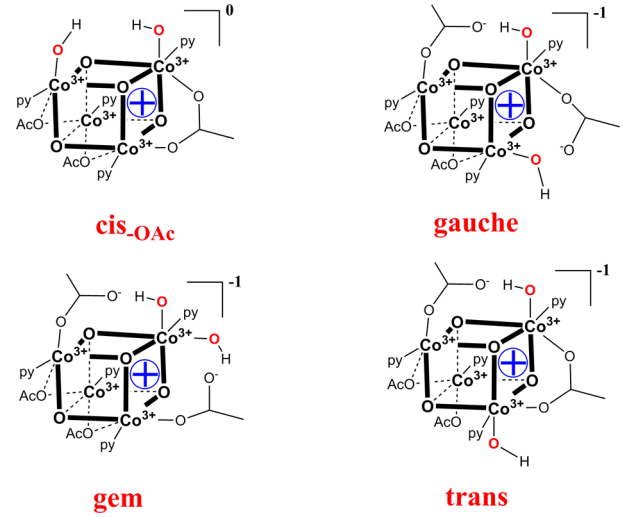

Figure 8. List of considered isomers of possible binding sites of second OH^-.

calculations find it weakly unfavorable to replace a second pyridine ligand from $Co_4(3,3,3,4)$ with OH^- (+0.07 eV) or H_2O (+0.05 eV). Thus, the cubium likely retains at least three pyridine ligands throughout the catalytic mechanism. This agrees with the studies of Bonchio et al., who observed a direct correlation of electron transfer rates with the Hammett values of pyridine substituents.[51]

We thus considered associative intermediates of general formula $[\mathbf{1A}(OH)_2]^{-1}$ in which a second OH^- has inserted into one of the remaining seven Co−acetate bonds (Figure 8). One-electron oxidation of all of these isomers by $\mathbf{1A}^+$ is energetically favorable by $1.25 - E^0 > 0.15$ eV, yielding a formal $Co_4(3,3,4,4)$ redox level. This oxidation level can also be represented as a Co^{3+}-bound peroxo in which the two bound OH^- are oxidized and deprotonated, but this structural rearrangement is only feasible if the activation energy barriers for each isomer can be surmounted. Peroxo formation is greatly disfavored for the *trans* and *gauche* isomers in the absence of rotational

DOI: 10.1021/jacs.5b09152
J. Am. Chem. Soc. 2015, 137, 15460−15468

possibilities, which we are pursuing further. For the *cis*-type isomers, the OH^- ligands are separated by ~2.6 Å; this distance does not allow any appreciable O−O bond formation energy. In contrast, the *gem*-dihydroxo intermediate coordinates both OH on one Co and should have the lowest activation barrier to the peroxo intermediate of all dihydroxo intermediates. Our calculations cannot distinguish a preference for *cis*- or *gem*-type intermediates, as these are isoenergetic in our most refined calculations to date (assuming four explicit water molecules in addition to the dielectric solvation model). Preliminary results also indicate similar stability of the ensuing peroxide-bound cubanes. Further, these intermediates are energetically degenerate (within <0.1 eV) with the corresponding oxo-aquo tautomers $[(\mathbf{1A}(O)(H_2O)]^0$ in triplet ground state in the dielectric solvation model (Figure S9). We note such intermediates require different O−O bond formation mechanisms, with the latter involving nucleophilic addition of a third OH^- to the $Co^V{=}O$. Both mechanisms have literature precedence, as water oxidation through a 1,1-*gem*-diol was proposed by Mattioli et al.,[63] while Wang and Van Voorhis[57] reported coupling via a 1,2-*cis*-diol.

While our calculations currently cannot distinguish between the *gem* and *cis* intermediates in terms of energy, future calculations to predict the activation barriers for O−O bond formation may resolve this question. However, our experimental data provide clear guidance on this question. Our NMR data show 0.5% (net) ligand dissociation occurs (carboxylate dissociation is required for the *cis* pathway), thus favoring the geminal pathway. Additional experimental evidence for the geminal pathway comes from our studies of the analogous cubium $\mathbf{1B}^{3+}$, as described next.

Reaction of $\mathbf{1B}^{3+}$ with Hydroxide. We pursued analogous experimental tests of cubium $\mathbf{1B}^{3+}$. This derivative features a more positively charged cubane coordinated by 4 bidentate bpy and 2 bidentate OAc^- ligands in trans geometry (Scheme 1). Consequently, DFT calculations predict higher OH^- affinity for this derivative, with formation of the positively charged $[cis\text{-}\mathbf{1B}(OH)_2]^+_{-OAc}$ complex favored by 0.30 eV relative to formation of the negatively charged $[cis\text{-}\mathbf{1A}(OH)_2]^{-1}_{-OAc}$ species. $\mathbf{1B}^{3+}$ shows a ~400 mV higher reduction potential than $\mathbf{1A}^+$ in acetonitrile,[54] but the measured electrochemical potentials are identical (1.25 V vs NHE) in >pH 4 water.[42,50] Carboxylate exchange is known for both cubanes,[35,54] and **1A** is known to bind water at these sites,[60,61] suggesting bound water may contribute to this change in oxidizing potential.

A reported synthesis was used to isolate $\mathbf{1B}(ClO_4)_3$ according to Christou et al.[34] To our knowledge, the EPR signal has not been previously published, but has been described as a broad resonance at g = 2.20 with no resolved hyperfine. Our EPR spectrum (Figure S7) confirms this description and identifies the ground-state spin S = 1/2. The shift of the g value (g > 2.0023) arising from Co spin−orbit coupling indicates a greater than half-filled $3d^n$ valence shell (n > 5). Analogous to $\mathbf{1A}^+$, the absence of resolved ^{59}Co hyperfine splitting indicates the hole is delocalized onto the four μ_3-oxos of the $[Co_4O_4]^{5+}$ core, and the average spin density on any one Co is <25%.

In sharp contrast to $\mathbf{1A}^+$, no O_2 is produced from the reaction between $\mathbf{1B}(ClO_4)_3$ and OH^-. This species does react but only CO_2 is produced, indicating bpy ligand oxidation. Bpy oxidation also occurs in pH neutral water: UV−vis spectroscopy of aqueous $\mathbf{1B}^{3+}$ solutions after aging for 1 h show 12 ± 3% reduction to cubane $\mathbf{1B}^{2+}$ with no production of O_2 (Figure S8). No evidence of any reaction was observed in acidic solution (pH 0−2).

We derive two conclusions from these results. First, $\mathbf{1B}(ClO_4)_3$ serves as a negative control in which the initial hydrolytic or oxidation intermediates are not reactive in water oxidation over bpy oxidation. Second, we infer one possible origin of the different water oxidation activities of $\mathbf{1A}^+$ and $\mathbf{1B}^{3+}$ as due to their different carboxylate stereochemistry. Only $\mathbf{1A}^+$ can form the *geminal*-1,1 intermediate, while both $\mathbf{1A}^+$ and $\mathbf{1B}^{3+}$ can form the *cis*-1,2 intermediates depicted in Figure 8.

DISCUSSION

The molecular Co_4O_4 cubane is inert for electrochemical oxidation of water to O_2 in aqueous phosphate buffer at pH 7.[59−61] This fact has been suggested by Nocera et al.[59] as evidence that the cubane core is not a direct catalyst for water oxidation, but rather breakdown products or other Co contaminants may have been the precatalysts that formed active centers. The evidence presented here and recently by others[60,61] has shown this first observation is true because water cannot bind to Co centers in the cubane **1A** in competition with Py, OAc^-, and phosphate ligands. However, when water is ionized to hydroxide, this stronger nucleophile is sufficient to form an inner-sphere association complex with **1A** in higher yield, which is a precatalyst to O_2 evolution. The results shown herein and by Tilley et al.[61] extend that strategy by starting with the cationic cubium $\mathbf{1A}^+$, thereby further favoring the association complex. Subsequent reaction with a second OH^- as shown kinetically[61] and indicated by our DFT calculations leads to an intermediate that can now be oxidized by $\mathbf{1A}^+$ resulting in O_2 evolution. This system may be analogous to that reported of Cronin et al., who observed O_2 evolution upon dissolution of heterogeneous Co^{IV}−oxides.[64]

In agreement with Tilley et al.,[61] our results find a reaction of stoichiometry $4\mathbf{1A}^+ + 4OH^- \rightarrow O_2 + 4\mathbf{1A} + 2H_2O$ with quantitative recovery of O_2 (75%, ref 61 vs 100%, here) and **1A** (99.5%). The O_2 product originates from OH^- and not bridging oxos, as evidenced by QTOF-MS and MIMS (>81% doubly labeled O_2). O_2 produced via outer-sphere oxidation of free hydroxide to $OH^\bullet$ radical (1.8−2.0 V) is not possible energetically. Rather, our calculations also agree that OH^- insertion into Co−OAc^- binding sites is energetically preferential, as also predicted by Li and Siegbahn.[56] We find that insertion of two OH^- into Co−OAc^- sites, forming either 1,1(*gem*)-dihydro or 1,2-dihydroxo intermediates, is an energetically favorable pathway to form species that, thermodynamically, can be oxidized by $\mathbf{1A}^+$ to yield either side-on ($\eta^{1,1}$-) or bridging ($\eta^{1,2}$-) peroxo intermediates, respectively.

Our kinetic studies, measured using saturating concentrations of OH^- and $\mathbf{1A}^+$, fit well a simple first-order molecularity in each (R^2 = 0.98), and no improvement to the fit is made by introducing a second-order term (R^2 = 0.98). However, Tilley et al.[61] reported a faster time resolution kinetic study using stopped flow UV−vis absorption, and showed the rate expression fits better to the sum of first- and second-order terms in $\mathbf{1A}^+$ when nonsaturating concentrations are used. Our first-order rate constant (1.1) compares exceptionally well to that obtained by Tilley et al. (0.8), confirming these studies are self-consistent. Neither we nor Tilley et al. have observed any reaction intermediate directly. The proposed reaction mechanism by both groups is kinetically identical, only differing in terms of the description of the later intermediates. Both

DOI: 10.1021/jacs.5b09152
J. Am. Chem. Soc. 2015, 137, 15460−15468

proposals involve associative addition of the first OH^- to $\mathbf{1A}^+$ yielding intermediate $[\mathbf{1A}(OH)]^0$.

The main mechanistic difference of our proposal as compared to Li and Siegbahn[56] and Tilley et al.[61] is that the second oxidation step to the formal $Co_4(3,3,4,4)$ cannot occur at the first hydroxide intermediate due to insufficient redox energy for $\mathbf{1A}^+/\mathbf{1A}$, but becomes favorable after a second OH^- associates. Second, we find (via EPR) that electron−hole delocalization is a required feature of the mixed valence states rather than localized Co oxidation states. These features are emphasized in our proposed mechanism (Scheme 2). Here, we

Scheme 2. Proposed Mechanism of Hydroxide Oxidation by Cubane Complexes, Building on Concepts from This Work and Elsewhere[54]

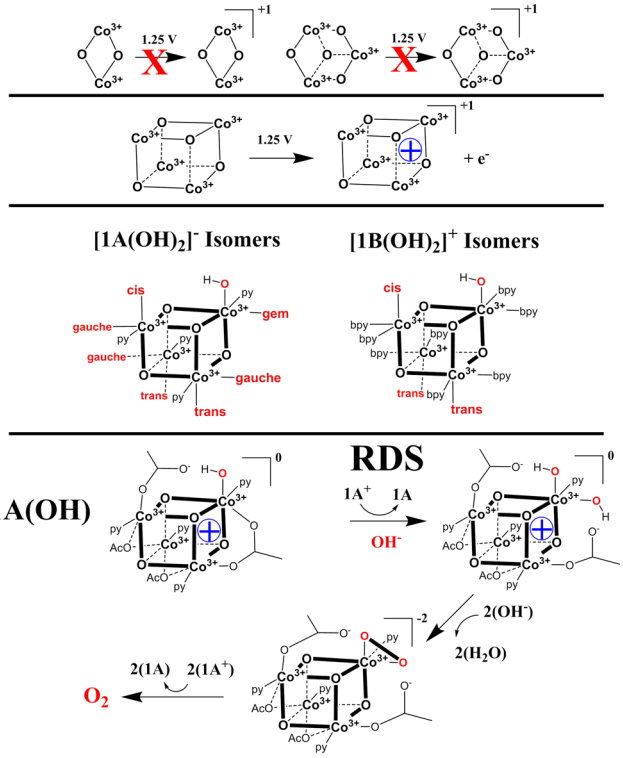

propose that OH^- addition and one-electron oxidation (by a second equivalent of $\mathbf{1A}^+$) forms the dihydroxo species, $[\mathbf{1A}(OH)_2]^0$, by concerted or stepwise reactions and is rate limiting for overall O_2 production.

We previously showed that neither trinuclear nor dinuclear Co(III) complexes prepared using the identical sets of ligands, py/OAc^- or bpy/OAc^-, exhibit activity in water oxidation.[54] This is attributed to their >0.8 V higher reduction potential for the mixed valence Co(IV)/Co(III) couples. These noncuboidal compounds lack the favorable delocalization energy unique to the molecular orbitals of the cubane topology, as evidenced both here and elsewhere by EPR spectroscopy.[44] Hence, the cubane structure allows stabilization of the $Co_4(3,3,4,4)$ oxidation state, from which a $Co_4(3,3,3,3)$-bound peroxide can be obtained. The production of O_2 from this step follows easily, as $\mathbf{1A}^+$ is capable of oxidizing hydrogen peroxide.[61]

Considering the absence of O_2 evolution from cubium $\mathbf{1B}^{3+}$, which lacks geminal OAc^- ligands, we strongly favor the *gem*-1,1-dihydroxo pathway over the *cis*-1,2-dihydroxo pathway for O_2 evolution by $\mathbf{1A}^+$. However, we cannot rule out other reasons for why $\mathbf{1B}^{3+}$ is a poorer precatalyst. Competition between oxidation of bpy (CO_2 evolution) and OH^- oxidation, or slow kinetics due to charge repulsion between 2+ and 3+ cations, could be two reasons why the yield of O_2 is zero.

With this mechanism established we can thus conclude that, under photochemical conditions using photogenerated oxidants ($Ru(bpy)_3^{3+}$, 1.26 V, and persulfate radical, 2.4 V), earlier reports[49−51,54] most likely observed a combination of O_2 produced catalytically from **1A** and Co^{2+} impurities. It is plausible that ligand dissociation to produce available water binding sites on cubane **1A** is more facile under illumination, rationalizing different observations seen between photochemical and electrochemical systems.[59] Precedence for this is known by the $Mn_4O_4(O_2PPh_2)_6$ cubane, which photodissociates phosphinate anion upon UV irradiation.[65−68] The apparent inactivity of a water oxidation catalyst candidate under one set of conditions thus cannot infer that the candidate will be inactive under all conditions.

Many observations reported here provide updated context for earlier reports[49−51,54] discussing catalysis from **1A**. Our data show 0.5% ligand loss following a single turnover of $\mathbf{1A}^+/OH^-$, in excellent agreement with literature showing <5% photodecomposition of **1A** after 6−12 turnovers using $Ru(bpy)_3^{3+}$ and persulfate radicals.[49] The lack of O_2 evolution at pH 7 in the absence of buffer in this latter system[54] is now rationalized by the insufficient concentration of necessary OH^- substrate.

Our kinetic results rationalize the previous observation[54] that $Ru(bpy)_3^{3+}$ alone (1.26 V) could not generate O_2 from **1A** and water. This observation was reinforced by electrochemical results of several groups[49,51,59] (as well as Figure 1), which show little to no water oxidation current at applied potentials in that region. As measured here, pseudo-first-order rate constants for hydroxide reaction with $\mathbf{1A}^+$ are on the order of 10^{-4}−10^{-3} s^{-1} (Figure 4). Rates of $Ru(bpy)_3^{3+}$ decomposition by OH^- promoted hydrolysis are on the order of 10^{-3}−10^{-2} s^{-1}, as measured by Mallouk et al.[69] Hence, hydroxide (if available) reacts with $Ru(bpy)_3^{3+}$ (typically in excess concentration) roughly an order of magnitude faster than with $\mathbf{1A}^+$. When considering that all previous studies have utilized pH 7−8 (=10^{-6}−10^{-7} M $[OH^-]$), millimolar concentrations of $\mathbf{1A}^+$ would yield rates approximately 10^{-9}−10^{-10} s^{-1} for O_2 evolution, as estimated by eq 2. Such rates are likely to be additionally affected by the presence of buffers, which have been reported to compete for cobalt binding sites.[70] In particular, phosphate has been shown to inactivate[71] and inhibit[20] homogeneous cobalt catalysts by binding at sites for substrate OH^-.

CONCLUSION

Effective heterogeneous oxidation catalysts such as spinel Co_3O_4 and cubic $LiCoO_2$ have lattices built around a Co_4O_4 cubane-type structure.[2,4,72] This architecture is known to be important to allow thermodynamically accessible oxidation to Co^{4+}, as evidenced by the favorable oxidation potentials of the molecular clusters, $\mathbf{1A}/\mathbf{1A}^+$ and $\mathbf{1B}^{2+}/\mathbf{1B}^{3+}$, in contrast to the much higher Co^{III}/Co^{IV} oxidation potentials (~1 V higher) for $[Co_3O_4]^{2+}$ and $[Co_2O_2]^+$ model complexes with identical ligands.[54] These heterogeneous catalysts, at an oxidizing potential of 1.26 V ($Ru(bpy)_3^{3+}$), have pseudo-first-order rate constants for O_2 evolution on the order of 10^{-2}−10^{-1}/s·Co (e.g, 0.019 for $LiCoO_2$,[4] 0.01 for Co_3O_4,[2] 0.5 for Co-M2P[15]).

With the assumption of rate laws similar to that reported here, the pseudo-first-order rate constants we obtain at 1.25 V

DOI: 10.1021/jacs.5b09152
J. Am. Chem. Soc. 2015, 137, 15460−15468

(10^{-4}–10^{-3}, Figure 4) indicate 10–1000× faster kinetics for water oxidation are afforded by efficient water/hydroxide binding. This comparison suggests that a molecular metal–oxo cubane architecture in a coordination environment of oxidatively stable ligands could achieve even faster turnover rates than homogeneous catalysts. While cubium $\mathbf{1B}^{3+}$ did not have stable organic ligand architecture, the acetates and pyridines are not oxidized in the case of $\mathbf{1A}^{+}$. Hence, this offers an optimistic future that molecular cobalt catalysts with organic ligands, if designed appropriately, may tolerate the harsh conditions needed to oxidize water and remain stable over useful lifetimes.

Last, when testing water oxidation catalysts with chemical oxidants, few are known[73] and each have trade-offs: for example, cerium ammonium nitrate has been challenged as noninnocent,[74] sodium periodate may donate substrate oxos, and $Ru(bpy)_3^{3+}$ is unstable. Here, pristine $\mathbf{1A}^{+}$ shows excellent aqueous stability at pH < 7 ($\mathbf{1B}^{3+}$ < pH 4). Cubium couples appear to be an innocent, outer-sphere one-electron redox mediator under acidic conditions.

EXPERIMENTAL SECTION

Materials and Methods. All solutions were prepared with reagent grade water (18 MΩ, Hydro Picopure). All solvents and reagents were reagent grade, purchased commercially, and used without further purification. $NaH^{13}C^{18}O_3$ bicarbonate was used to induce formation of $^{18}OH^{-}$ in experiments requiring isotopic labeling. ^{18}O water was purchased as 97% from Aldrich or 98% from Icon Isotopes. UV–vis spectra were recorded on an HP-8452A Diode Array spectrophotometer in standard 1 cm path length quartz cells. EPR spectra were recorded on a Bruker ESP300 spectrometer equipped with Oxford cryostat model 900 at 10 K. Samples were glasses of $\mathbf{1A}^{+}$ in acetonitrile and $\mathbf{1B}^{+}$ in 1 M H_2SO_4. A CH Instruments Electrochemical Workstation was used for exhaustive electrolysis experiments.

A Clark-type oxygen electrode (Hansatek Ltd.) was used to obtain oxygen evolution data, and calibrated daily using N_2 deoxygenated and oxygen saturated atmospheric solutions. Clark electrode experiments were performed by monitoring the addition of 20 μL of 1 M NaOH to 500 μL of 95/5 H_2O/CH_3CN solutions of $\mathbf{1A}^{+}$. The initial rates were obtained by determining the slope over the beginning linear region (~10 s) of O_2 evolution.

Gas chromatography data were recorded on a PerkinElmer Clarus 680 GC with a TCD detector (Ar carrier gas) operating at 40 °C (O_2) or 200 °C (CO_2). Gas chromatography experiments monitored the addition of 200 μL of Ar-degassed 0.1 M NaOH to solid powders of $\mathbf{1A}^{+}$ or $\mathbf{1B}^{3+}$ in Ar-degassed 2 mL vials, and were adjusted using the N_2 signal as a control.

Membrane inlet mass spectroscopy data were taken with a Stanford Research Systems CIS100 residual gas analyzer. A 1/16" capillary partially submerged in a dry ice/ethylene glycol/ethanol trap at −40 °C was used to connect the CIS to a KF/Swagelok adapter, in which sat a porous polyethylene support, a 12.5 μm Teflon membrane (Hansatech), and an O-ring. This assembly was clamped to the KF connection of a glass reaction vessel. Solid $\mathbf{1A}^{+}$ and ^{18}O bicarbonate were placed on top of the membrane while the vessel was Ar-purged, and ^{18}O was Ar-purged in its container as delivered. When ^{18}O water was added by syringe, nitrogen, CO_2 (labeled and unlabeled), and argon were monitored in addition to the O_2 isotopes as control signals; the $^{32}O_2$ and $^{34}O_2$ signals were adjusted from the residual N_2 signal in the resulting data. The $^{36}O_2$ signal was adjusted from the background Ar signal in the resulting data. All O_2 signals adjust for separate background signals before injection. For MS data >100 amu, spectra were recorded by direct injection of nM samples via syringe pump into an Agilent 6510 QTOF LC/MS running in dual ESI mode.

Syntheses. **1A** was prepared as previously described.[49,54] Purification was performed by collecting the first, green fraction off a column of silica gel using 5% methanol/dichloromethane mobile phase. $\mathbf{1AClO_4}$ ($\mathbf{1A}^{+}$) was made by bulk electrolysis (1.1–1.2 V) of a 0.4 M $LiClO_4/CH_3CN$ solution of **1A**, followed by reduction of solvent volume to ~5 mL by rotary evaporation, addition of water (~35 mL), and overnight refrigeration, giving a precipitate collected by filtration in 10–15% yield. A porous carbon rod (working), Ti wire (counter), and silver wire (pseudoreference) were used as electrodes; the latter two electrodes were compartmentalized in fritted glass tubes (Ace glass) filled only with blank electrolyte (no cobalt). $\mathbf{1A}^{+}$ as the PF_6 salt was prepared exactly as described in ref 59.

$\mathbf{1B}^{2+}$ as a perchlorate salt was prepared as described[54] as the salt that precipitates following CH_3CN electrolysis of $\mathbf{1B}^{2+}$ at 1.5 V vs Ag pseudoreference.

Computational Details. All of the calculations have been performed by the Gaussian 09 program package.[75] We optimized all of the molecular structures using the B3LYP exchange-correlation functional[76] and a 6-311G* basis set[77,78] in vacuo. The solvation effects are evaluated by the conductor-like polarizable continuum model (C-PCM),[79,80] using acetonitrile as a solvent. To calculate the energetics of the reaction pathways, we used fragments (OH^{-}, OAc^{-}, and Py) including four explicit water molecules in acetonitrile.

ASSOCIATED CONTENT

Supporting Information

The Supporting Information is available free of charge on the ACS Publications website at DOI: 10.1021/jacs.5b09152.

Nine figures including QTOF-MS and raw DFT data (PDF)

AUTHOR INFORMATION

Corresponding Author

*dismukes@rutgers.edu

Notes

The authors declare no competing financial interest.

ACKNOWLEDGMENTS

This work was supported by the Air Force Office of Scientific Research (FA9550-11-1-0231). Fellowships were provided by NSF-IGERT (P.F.S., DGE 0903675), NSF CLP no. 1213772 (S.K.), Rutgers University (A.B.L.), the Lawrenceville School, Lawrenceville, NJ (L.H.), CAPES Brazil 13386/13-1 (K.U.D.C), and BASF (V.S.). We are grateful to Drs. A. Ermakov, G. K. Kumaraswamy, and A. Tyryshkin for instrumentation support and to Dr. Y. Geletii, Dr. M. Symes, G. Gardner, and C. Kaplan for helpful discussions.

REFERENCES

(1) Shafirovich, V. Y.; Strelets, V. V. *Nouv. J. Chim.* **1977**, *2*, 199–201.
(2) Jiao, F.; Frei, H. *Angew. Chem., Int. Ed.* **2009**, *48*, 1841–1844.
(3) Brunschwig, B. S.; Chou, M. H.; Creutz, C.; Ghosh, P.; Sutin, N. *J. Am. Chem. Soc.* **1983**, *105*, 4832–4833.
(4) Gardner, G. P.; Go, Y. B.; Robinson, D. M.; Smith, P. F.; Hadermann, J.; Abakumov, A.; Greenblatt, M.; Dismukes, G. C. *Angew. Chem.* **2012**, *124*, 1648–1651.
(5) Suzuki, O.; Takahashi, M.; Fukunaga, T.; Kuboyama, J. U.S. Patent 3399966, 1968.
(6) El Wakkad, S. E. S.; Hickling, A. *Trans. Faraday Soc.* **1950**, *46*, 820–824.
(7) Kanan, M. W.; Nocera, D. G. *Science* **2008**, *321*, 1072–1075.
(8) Hutchings, G. S.; Zhang, Y.; Li, J.; Yonemoto, B. T.; Zhou, X.; Zhu, K.; Jiao, F. *J. Am. Chem. Soc.* **2015**, *137*, 4223–4229.
(9) Gerken, J. B.; McAlpin, J. G.; Chen, J. Y. C.; Rigsby, M. L.; Casey, W. H.; Britt, R. D.; Stahl, S. S.; Rigsby, L.; Casey, W. H.; Britt, R. D.; Stahl, S. S. *J. Am. Chem. Soc.* **2011**, *133*, 14431–14442.
(10) Nocera, D. G. *Acc. Chem. Res.* **2012**, *45*, 767–776.

DOI: 10.1021/jacs.5b09152
J. Am. Chem. Soc. 2015, 137, 15460–15468

(11) Risch, M.; Ringleb, F.; Chernev, P.; Zaharieva, I.; Dau, H. *Energy Environ. Sci.* **2015**, *8*, 661−674.
(12) Risch, M.; Klingan, K.; Ringleb, F.; Chernev, P.; Zaharieva, I.; Fischer, A.; Dau, H. *ChemSusChem* **2012**, *5*, 542−549.
(13) Du, P.; Kokhan, O.; Chapman, K. W.; Chupas, P. J.; Tiede, D. M. *J. Am. Chem. Soc.* **2012**, *134*, 11096−11099.
(14) Zhong, M.; Hisatomi, T.; Kuang, Y.; Zhao, J.; Liu, M.; Iwase, A.; Jia, Q.; Nishiyama, H.; Minegishi, T.; Nakabayashi, M.; Shibata, N.; Niishiro, R.; Katayama, C.; Shibano, H.; Katayama, M.; Kudo, A.; Yamada, T.; Domen, K. *J. Am. Chem. Soc.* **2015**, *137*, 5053−5060.
(15) Koroidov, S.; Anderlund, M. F.; Styring, S.; Thapper, A.; Messinger, J. *Energy Environ. Sci.* **2015**, *8*, 2492−2503.
(16) Li, Y.; Zhang, L.; Torres-Pardo, A.; González-Calbet, J. M.; Ma, Y.; Oleynikov, P.; Terasaki, O.; Asahina, S.; Shima, M.; Cha, D.; Zhao, L.; Takanabe, K.; Kubota, J.; Domen, K. *Nat. Commun.* **2013**, *4*, 2566.
(17) Kanan, M. W.; Surendranath, Y.; Nocera, D. G. *Chem. Soc. Rev.* **2009**, *38*, 109−114.
(18) Zhong, D. K.; Cornuz, M.; Sivula, K.; Gratzel, M.; Gamelin, D. R. *Energy Environ. Sci.* **2011**, *4*, 1759−1764.
(19) Han, X. B.; Zhang, Z. M.; Zhang, T.; Li, Y. G.; Lin, W.; You, W.; Su, Z. M.; Wang, E. B. *J. Am. Chem. Soc.* **2014**, *136*, 5359−5366.
(20) Wang, D.; Groves, J. T. *Proc. Natl. Acad. Sci. U. S. A.* **2013**, *110*, 15579−15584.
(21) Wasylenko, D. J.; Ganesamoorthy, C.; Borau-Garcia, J.; Berlinguette, C. P. *Chem. Commun.* **2011**, *47*, 4249−4251.
(22) Dogutan, D. K.; McGuire, R.; Nocera, D. G. *J. Am. Chem. Soc.* **2011**, *133*, 9178−9180.
(23) Shevchenko, D.; Anderlund, M. F.; Thapper, A.; Styring, S. *Energy Environ. Sci.* **2011**, *4*, 1284−1287.
(24) Rigsby, M. L.; Mandal, S.; Nam, W.; Spencer, L. C.; Llobet, A.; Stahl, S. S. *Chem. Sci.* **2012**, *3*, 3058.
(25) Evangelisti, F.; Güttinger, R.; Moré, R.; Luber, S.; Patzke, G. R. *J. Am. Chem. Soc.* **2013**, *135*, 18734−18737.
(26) Yin, Q.; Tan, J. M. J. M.; Besson, C.; Geletii, Y. V.; Musaev, D. G.; Kuznetsov, A. E.; Luo, Z.; Hardcastle, K. I.; Hill, C. L. *Science (Washington, DC, U. S.)* **2010**, *328*, 342−345.
(27) Pizzolato, E.; Natali, M.; Posocco, B.; Montellano Lopez, A.; Bazzan, I.; Di Valentin, M.; Galloni, P.; Conte, V.; Bonchio, M.; Scandola, F.; Sartorel, A.; Montellano López, A. *Chem. Commun.* **2013**, *49*, 9941−9943.
(28) Leung, C.-F.; Ng, S.-M.; Ko, C.-C.; Man, W.-L.; Wu, J.; Chen, L.; Lau, T.-C. *Energy Environ. Sci.* **2012**, *5*, 7903.
(29) Lv, H.; Song, J.; Geletii, Y. V.; Vickers, J. W.; Sumliner, J. M.; Musaev, D. G.; Kögerler, P.; Zhuk, P. F.; Bacsa, J.; Zhu, G.; Hill, C. L. *J. Am. Chem. Soc.* **2014**, *136*, 9268−9271.
(30) Swiegers, G. F.; Clegg, J. K.; Stranger, R. *Chem. Sci.* **2011**, *2*, 2254−2262.
(31) Sartorel, A.; Bonchio, M.; Campagna, S.; Scandola, F. *Chem. Soc. Rev.* **2013**, *42*, 2262−2280.
(32) Dismukes, G. C.; Brimblecombe, R.; Felton, G. A. N.; Pryadun, R. S.; Sheats, J. E.; Spiccia, L.; Swiegers, G. F. *Acc. Chem. Res.* **2009**, *42*, 1935−1943.
(33) Blakemore, J. D.; Crabtree, R. H.; Brudvig, G. W. *Chem. Rev.* **2015**, 150720112150009.
(34) Dimitrou, K.; Brown, A. D.; Concolino, T. E.; Rheingold, A. L.; Christou, G. *Chem. Commun.* **2001**, 1284−1285.
(35) Dimitrou, K.; Folting, K.; Streib, W. E.; Christou, G. *J. Am. Chem. Soc.* **1993**, *115*, 6432−6433.
(36) Dimitrou, K.; Sun, J.-S. S.; Folting, K.; Christou, G. *Inorg. Chem.* **1995**, *34*, 4160−4166.
(37) Dimitrou, K.; Folting, K.; Streib, W. E.; Christou, G. *J. Chem. Soc., Chem. Commun.* **1994**, *838*, 1385−1386.
(38) Chakrabarty, R.; Bora, S. J.; Das, B. K. *Inorg. Chem.* **2007**, *46*, 9450−9462.
(39) Chakrabarty, R.; Sarmah, P.; Saha, B.; Chakravorty, S.; Das, B. K. *Inorg. Chem.* **2009**, *48*, 6371−6379.
(40) Sarmah, P.; Chakrabarty, R.; Phukan, P.; Das, B. K. *J. Mol. Catal. A: Chem.* **2007**, *268*, 36−44.
(41) Das, B. K.; Chakrabarty, R. *J. Chem. Sci.* **2011**, *123*, 163−173.
(42) Symes, M. D.; Surendranath, Y.; Lutterman, D. a.; Nocera, D. G. *J. Am. Chem. Soc.* **2011**, *133*, 5174−5177.
(43) Symes, M. D.; Lutterman, D. A.; Teets, T. S.; Anderson, B. L.; Breen, J. J.; Nocera, D. G. *ChemSusChem* **2013**, *6*, 65−69.
(44) McAlpin, J. G.; Stich, T. A.; Ohlin, C. A.; Surendranath, Y.; Nocera, D. G.; Casey, W. H.; Britt, R. D. *J. Am. Chem. Soc.* **2011**, *133*, 15444−15452.
(45) Stich, T.; Krzystek, J.; Mercardo, B. Q.; McAlpin, J. G.; Ohlin, C. A.; Olmstead, M. M.; Casey, W. H.; Britt, R. D. *Polyhedron* **2013**, *64*, 304−307.
(46) McAlpin, J. G.; Surendranath, Y.; Dincă, M.; Stich, T. A.; Stoian, S. A.; Casey, W. H.; Nocera, D. G.; Britt, R. D. *J. Am. Chem. Soc.* **2010**, *132*, 6882−6883.
(47) Beattie, J. K.; Hambley, T. W.; Klepetko, J. a.; Masters, A. F.; Turner, P. *Polyhedron* **1998**, *17*, 1343−1354.
(48) Sumner, C. E. *Inorg. Chem.* **1988**, *27*, 1320−1327.
(49) McCool, N. S.; Robinson, D. M.; Sheats, J. E.; Dismukes, G. C. *J. Am. Chem. Soc.* **2011**, *133*, 11446−11449.
(50) La Ganga, G.; Puntoriero, F.; Campagna, S.; Bazzan, I.; Berardi, S.; Bonchio, M.; Sartorel, A.; Natali, M.; Scandola, F. *Faraday Discuss.* **2012**, *155*, 177.
(51) Berardi, S.; Natali, M.; Bazzan, I.; Puntoriero, F.; Sartorel, A.; Scandola, F.; Campagna, S.; Bonchio, M. *J. Am. Chem. Soc.* **2012**, *134*, 11104−11107.
(52) Zhang, B.; Li, F.; Yu, F.; Wang, X.; Zhou, X.; Li, H.; Jiang, Y.; Sun, L. *ACS Catal.* **2014**, *4*, 804−809.
(53) Zhou, X.; Li, F.; Li, H.; Zhang, B.; Yu, F.; Sun, L. *ChemSusChem* **2014**, *7*, 2453−2456.
(54) Smith, P. F.; Kaplan, C.; Sheats, J. E.; Robinson, D. M.; McCool, N. S.; Mezle, N.; Dismukes, G. C. *Inorg. Chem.* **2014**, *53*, 2113−2121.
(55) La Ganga, G.; Nardo, V. M.; Cordaro, M.; Natali, M.; Vitale, S.; Licciardello, A.; Nastasi, F.; Campagna, S. *Dalt. Trans* **2014**, *43*, 14926−14930.
(56) Li, X.; Siegbahn, P. E. M. *J. Am. Chem. Soc.* **2013**, *135*, 13804−13813.
(57) Wang, L. P.; Van Voorhis, T. *J. Phys. Chem. Lett.* **2011**, *2*, 2200−2204.
(58) Fernando, A.; Aikens, C. M. *J. Phys. Chem. C* **2015**, *119*, 11072−11085.
(59) Ullman, A. M.; Liu, Y.; Huynh, M.; Bediako, D. K.; Wang, H.; Anderson, B. L.; Powers, D. C.; Breen, J. J.; Abruña, H. D.; Nocera, D. G. *J. Am. Chem. Soc.* **2014**, *136*, 17681−17688.
(60) Sartorel, A.; Genoni, A.; LaGanga giuseppina; Volpe, A.; Puntoriero, F.; Di Valentin, M.; Bonchio, M.; Natali, M. *Faraday Discuss.* **2015**, DOI: 10.1039/C5FD00076A.
(61) Nguyen, A. I.; Ziegler, M. S.; Oña-Burgos, P.; Sturzbecher-Hohne, M.; Kim, W.; Bellone, D. E.; Tilley, T. D. *J. Am. Chem. Soc.* **2015**, *137*, 12865−12872.
(62) Wu, J. Z.; Sellitto, E.; Yap, G. P. A.; Sheats, J.; Dismukes, G. C. *Inorg. Chem.* **2004**, *43*, 5795−5797.
(63) Mattioli, G.; Giannozzi, P.; Amore Bonapasta, A.; Guidoni, L. *J. Am. Chem. Soc.* **2013**, *135*, 15353−15363.
(64) Bloor, L. G.; Molina, P. I.; Symes, M. D.; Cronin, L. *J. Am. Chem. Soc.* **2014**, *136*, 3304−3311.
(65) Ruettinger, W.; Yagi, M.; Wolf, K.; Bernasek, S.; Dismukes, G. C. *J. Am. Chem. Soc.* **2000**, *122*, 10353−10357.
(66) Wu, J. Z.; De Angelis, F.; Carrell, T. G.; Yap, G. P. A.; Sheats, J.; Car, R.; Dismukes, G. C. *Inorg. Chem.* **2006**, *45*, 189−195.
(67) Brimblecombe, R.; Swiegers, G. F.; Dismukes, G. C.; Spiccia, S. *Angew. Chem., Int. Ed.* **2008**, *47*, 7335−7338.
(68) Brimblecombe, R.; Kolling, D. R. J.; Bond, A. M.; Dismukes, G. C.; Spiccia, L.; Swiegers, G. F. *Inorg. Chem.* **2009**, *48*, 7269−7279.
(69) Hara, M.; Waraksa, C. C.; Lean, J. T.; Lewis, B. A.; Mallouk, T. E. *J. Phys. Chem. A* **2000**, *104*, 5275−5280.
(70) Liu, H.; Schilling, M.; Yulikov, M.; Luber, S.; Patzke, G. R. *ACS Catal.* **2015**, *5*, 4994−4999.
(71) Davenport, T. C.; Ahn, H. S.; Ziegler, M. S.; Tilley, T. D. *Chem. Commun.* **2014**, *50*, 6326−6329.

DOI: 10.1021/jacs.5b09152
J. Am. Chem. Soc. 2015, 137, 15460−15468

(72) Cady, C. W.; Gardner, G.; Maron, Z. O.; Retuerto, M.; Go, Y. B.; Segan, S.; Greenblatt, M.; Dismukes, G. C. *ACS Catal.* **2015**, *5*, 3403−3410.
(73) Parent, A. R.; Crabtree, R. H.; Brudvig, G. W. *Chem. Soc. Rev.* **2013**, *42*, 2247−2252.
(74) Demars, T. J.; Bera, M. K.; Seifert, S.; Antonio, M. R.; Ellis, R. J. *Angew. Chem., Int. Ed.* **2015**, *54*, 7534−7538.
(75) Frisch, M. J.; Trucks, G. W.; Schlegel, H. B.; Scuseria, G. E.; Robb, M. A.; Cheeseman, J. R.; Scalmani, G.; Barone, V.; Mennucci, B.; Petersson, G. A.; Nakatsuji, H.; Caricato, M.; Li, X.; Hratchian, H. P.; Izmaylov, A. F.; Bloino, J.; Zheng, G.; Sonnenberg, J. L.; Hada, M.; Ehara, M.; Toyota, K.; Fukuda, R.; Hasegawa, J.; Ishida, M.; Nakajima, T.; Honda, Y.; Kitao, O.; Nakai, H.; Vreven, T.; Montgomery, J. A., Jr.; Peralta, J. E.; Ogliaro, F.; Bearpark, M.; Heyd, J. J.; Brothers, E.; Kudin, K. N.; Staroverov, V. N.; Kobayashi, R.; Normand, J.; Raghavachari, K.; Rendell, A.; Burant, J. C.; Iyengar, S. S.; Tomasi, J.; Cossi, M.; Rega, N.; Millam, J. M.; Klene, M.; Knox, J. E.; Cross, J. B.; Bakken, V.; Adamo, C.; Jaramillo, J.; Gomperts, R.; Stratmann, R. E.; Yazyev, O.; Austin, A. J.; Cammi, R.; Pomelli, C.; Ochterski, J. W.; Martin, R. L.; Morokuma, K.; Zakrzewski, V. G.; Voth, G. A.; Salvador, P.; Dannenberg, J. J.; Dapprich, S.; Daniels, A. D.; Farkas, Ö; Foresman, J. B.; Ortiz, J. V.; Cioslowski, J.; Fox, D. J. *Gaussian 09*, revision A.1; Gaussian, Inc.: Wallingford, CT, 2009.
(76) Becke, A. D. *J. Chem. Phys.* **1993**, *98*, 5648−5652.
(77) McLean, A. D.; Chandler, G. S. *J. Chem. Phys.* **1980**, *72*, 5639−5648.
(78) Krishnan, R.; Binkley, J. S.; Seeger, R.; Pople, J. A. *J. Chem. Phys.* **1980**, *72*, 650−654.
(79) Cossi, M.; Rega, N.; Scalmani, G.; Barone, V. *J. Comput. Chem.* **2003**, *24*, 669−681.
(80) Cossi, M.; Barone, V. *J. Chem. Phys.* **2001**, *115*, 4708−4717.

DOI: 10.1021/jacs.5b09152
J. Am. Chem. Soc. 2015, 137, 15460−15468